

Molecular determinants of ligand binding to H₄R species variants

Herman D. Lim^{*}, Chris de Graaf^{*}, Wen Jiang, Payman Sadek, Patricia M. McGovern, Enade P. Istyastono, Remko A. Bakker¹, Iwan J.P. de Esch, Robin L. Thurmond, and Rob Leurs

Leiden/Amsterdam Center for Drug Research, Division of Medicinal Chemistry, Faculty of Science, VU University Amsterdam, De Boelelaan 1083, 1081 HV Amsterdam, The Netherlands (HDL, CdeG, EPI, PS, RAB, IdeE, RL).

Johnson & Johnson Pharmaceutical Research and Development, LLC, 3210 Merryfield Row, San Diego, CA 92121 (WJ, PMM, RLT)

MOL #63040

Running title:

Molecular determinants of ligand binding to H₄R species variants

Corresponding author:

Prof. Dr. Rob Leurs

Leiden/Amsterdam Center for Drug Research, Division of Medicinal Chemistry, Faculty of Science, VU University Amsterdam, De Boelelaan 1083, 1081 HV Amsterdam, The Netherlands.

Tel.: +31-20-5987600

Fax.: +31-20-5987610

E-mail: r.leurs@few.vu.nl

Number of text pages	: 31
Number of tables	: 2
Number of figures	: 8
Number of words in abstract	: 158 (max. 250)
Number of words in introduction	: 579 (max. 750)
Number of words in discussion	: 1473 (max. 1500)

List of nonstandard abbreviations :

ADRB2, β_2 adrenergic receptor; GPCR, G protein-couple receptor; H₁R, histamine H₁ receptor; H₂R, histamine H₂ receptor; H₃R, histamine H₃ receptor; H₄R, histamine H₄ receptor; TM, transmembrane; EL2, second extracellular loop; SDM, site-directed mutagenesis.

Recommended section: Cellular and Molecular

ABSTRACT

The histamine H₄ receptor (H₄R) is the latest identified histamine receptor that is emerging as a potential drug target for inflammatory diseases. Animal models are employed to validate this potential drug target. Concomitantly, various H₄R orthologs have been cloned, including the human, mouse, rat, guinea pig, monkey, pig, and dog H₄R. In this paper, we expressed all these H₄R orthologs in HEK 293T cells and compared their interactions with currently used standard H₄R ligands, including the H₄R agonists histamine, 4-methylhistamine, VUF 8430, the H₄R antagonists JNJ 7777120 and VUF 6002, and the inverse H₄R agonist thioperamide. Most of the evaluated ligands display significantly different affinities at the different H₄R orthologs. These “natural mutants” of H₄R were used to study ligand-receptor interactions using chimeric human-pig-human and pig-human-pig H₄R proteins and site-directed mutagenesis. Our results are a useful reference for ligand selection for studies in animal models of diseases and offer new insights in the understanding of H₄R-ligand receptor interactions.

MOL #63040

INTRODUCTION

The histamine H₄ receptor (H₄R) is the latest identified member of the four known histamine receptor subtypes (Hough, 2001), which all belong to the family of G-protein coupled receptors (GPCRs). In view of the success of the histamine H₁ receptor (H₁R) and the histamine H₂ receptor (H₂R) as drug targets for the treatment of allergic conditions and gastric ulcers, respectively (Parsons and Ganellin, 2006), and the ongoing clinical trials of histamine H₃ receptor (H₃R) antagonists for CNS applications (Celanire et al., 2005), expectations for drugs targeting the H₄R are high (Smits et al., 2009). The H₄R is mainly present in leukocytes and mast cells, which are important components of the body's defense system (Liu et al., 2001a; Oda et al., 2000). A growing body of evidence implicates the H₄R in the regulation of the immune system, such as chemotaxis of eosinophils, mast cells, and monocyte-derived dendritic cells and modulation of chemical mediator production, such as leukotriene B₄, IL16, and other interleukins (Thurmond et al., 2008; Takeshita et al., 2003). These preclinical studies support the view that H₄R is a potential new drug target for inflammatory diseases, such as allergic asthma and rheumatoid arthritis (Thurmond et al., 2008).

Translational preclinical animal models are still crucial to predict the therapeutic potential of newly developed ligands in humans. Therefore, to study therapeutic effects of H₄R ligands in animal models of disease, it is important to characterize the H₄R of the corresponding species. For several GPCRs, including the H₃R, significant species differences are known and have seriously hampered drug discovery efforts (Hancock, 2006; Maconi et al., 2002; Oksenberg et al., 1992; Reinhart et al., 2004). Various species orthologs of H₄R were promptly cloned based on their homology to the human H₄R sequence (Oda et al., 2000), including those of mouse, rat, guinea pig, pig, monkey (*Macaca fascicularis*), and dog (Jiang et al., 2008; Liu et al., 2001b; Oda et al., 2002; Oda et al., 2005). The H₄R species variants show relatively low homology to the human H₄R (65-71%), except for the monkey

H₄R that shows an overall amino acid homology of 91% (Figure 1). The sequence differences of human, rat and mouse H₄R have been reported to result in significant differences in the affinity for the endogenous agonist histamine (Liu et al., 2001b). Detailed analysis of the differences in receptor structure resulted in the identification of F169^{45,55} in the second extracellular loop as one of the amino acid residues responsible for the mouse/human species difference in ligand binding (Lim et al. 2008).

In view of the relatively wide divergence in amino acid sequence among the various H₄R species orthologs (which can be considered as “natural mutagenesis”) we have extensively and systematically investigated this issue by expressing the human, monkey, pig, dog, guinea-pig, mouse and rat H₄R in HEK 293T cells and evaluated the interactions of the various H₄R proteins with a set of reference H₄R ligands that have been used in H₄R studies, including the H₄R agonists histamine, 4-methylhistamine (Lim et al., 2005), VUF 8430 (Lim et al., 2006), clozapine, and clobenpropit (Buckland et al., 2003), the H₄R antagonists JNJ 7777120 (Thurmond et al., 2004) and VUF 6002 (Terzioglu et al., 2004; Venable et al., 2005), and the H₄R inverse agonist thioperamide (Takeshita et al., 2003). Using chimeric human-pig-human and pig-human-pig H₄R proteins and site-directed mutagenesis (SDM) in combination with *in silico* modeling studies, we investigated the ligand-receptor interactions in detail and systematically identified key residues responsible for observed ligand dependent species differences.

MOL #63040

METHODS

Materials. Dulbecco's modified Eagle medium (DMEM), penicillin and streptomycin were purchased from Invitrogen Life Technologies (Merelbeke, Belgium). Cell culture plastic wares were obtained from Greiner Bio-one (Wemmel, Belgium). Tris base was purchased from AppliChem (Darmstadt, Germany). Linear 25-kDa polyethyleneimine (PEI) was obtained from Polyscience, Inc. (USA). Histamine dihydrochloride, clozapine, and branched 750 kDa PEI were purchased from Sigma (USA), while VUF 8430 (guanidinyethyl isothiourea), thioperamide maleate, clobenpropit dihydrochloride, JNJ 7777120 (1-[(5-chloro-1H-indol-2-yl)carbonyl]-4-methylpiperazine), and VUF 6002 (1-[(5-chloro-1H-benzimidazol-2-yl)carbonyl]-4-methylpiperazine) were synthesized at the Department of Medicinal Chemistry, Vrije Universiteit Amsterdam. [³H]Histamine (18.10 Ci/mmol) was purchased from Perkin-Elmer Life Science, Inc. (USA). Oligonucleotides primers for PCR were synthesized by Isogen Bioscience (Maarsen, The Netherlands). Endonuclease restriction enzymes, T₄ DNA ligase, and *Pfu* DNA polymerase were from MBI Fermentas (St. Leon-Rot, Germany).

DNA constructs and site-directed mutagenesis. The wild type human H₄R cDNA cloned in pcDNA3.1 was purchased from Missouri S & T resource center (in Rollo, MO). The cDNA was subcloned into a mammalian expression vector pcDEF3 (a gift from Dr. J. Langer) at *Bam*HI and *Xba*I sites. The cDNA encoding the pig H₄R that was a gift from Yamanouchi Pharmaceuticals (Japan) (Oda et al., 2002) was subcloned in pcDEF3. The cDNAs of the other H₄R species variants were synthesized by HD Biosciences Co., Ltd. (Shanghai, China) according to the sequences in the GeneBank (XM_547634 for dog, AAK97379 for guinea pig, BAE16558 for monkey *Macaca fascicularis*, NP_694727 for mouse, NP_571984 for rat H₄R, and cloned in pcDEF₃. All the H₄R cDNAs contain a Kozak sequence (GCCACC)

MOL #63040

before the start codon ATG. The plasmids were amplified in *E. coli* JM109 (Promega, USA) and purified using Nucleobond AX columns (Macherey-Nagel, Germany). Chimeric receptor constructs were created by exchanging the domain between the DRY motif at the bottom of TM3 (*Cla*I restriction site in the cDNA) and residue Glu5.46 in TM5 (*Eco*RI restriction site in the cDNA) of the human H₄R with that of the pig H₄R (resulting in the chimeric receptor HPH, after human-pig-human) and the corresponding domain of pig H₄R with that of the human H₄R (resulting in the PHP chimera, after pig-human-pig). Due to the presence of a *Eco*RI binding site in the pig H₄R cDNA region corresponding to proximity of N- and C-termini, we used PCR to facilitate construction of the latter chimera. Site-directed mutagenesis was performed by PCR using mutant oligonucleotide primers and verified by sequencing analysis.

Cell culture and transfection. HEK 293T cells were maintained in Dulbecco's modified Eagle medium (DMEM) supplemented with 10% fetal bovine serum (FBS) and 50 IU/ml penicillin, and 50 µg/ml streptomycin in a 5% CO₂ and 95% humidified atmosphere at 37°C. For transfections, 5 µg of receptor plasmid was mixed in 0.5 ml serum-free DMEM with 25 µl of 1 mg/ml 25 kDa linear polyethyleneimine (PEI). The mixture was incubated for 5-10 min at room temperature before it was added onto subconfluent HEK 293T cell monolayer culture submerged in 5 ml fresh culture medium. Transfected cells were detached from the plastic surface two days after transfection using 5 ml/dish phosphate buffered saline containing 1 mM EDTA and collected as pellet by centrifugation at 200xg for 3 minutes. The pellets were stored at -20°C until use.

[³H]Histamine binding assay. Radioligand binding assays were performed using homogenized transfected cells in 50 mM Tris-HCl binding buffer (pH 7.4 at room

MOL #63040

temperature) in a total assay volume of 200 μ l. Saturation binding analysis was performed using different concentrations of [3 H]histamine (18.10 Ci/mmol) in the absence and presence of 3-10 μ M JNJ 7777120. For displacement studies, cell homogenates were typically co-incubated at different concentrations of ligands in the presence of approximately 7 to 20 nM [3 H]histamine, in a total volume of 200 μ l. The reaction mixtures were incubated for 1 hour at room temperature (22°C), harvested on 96-well glass fiber C plates (Perkin-Elmer Life and Analytical Sciences, Inc., USA) that were pretreated with 0.3% PEI, followed by washing for 3 times using ice-cold 50 mM Tris-HCl buffer (pH 7.4 at 4°C). The radioactivity retained on the filters was measured by liquid scintillation counting. The equilibrium dissociation constant (K_D) and inhibition constant (K_i) values were calculated by non-linear regressions for a single binding site model using Graphpad Prism 4.0 (Graphpad Software, Inc., CA, USA).

Residue numbering and nomenclature. The Ballesteros-Weinstein residue numbering scheme (Ballesteros and Weinstein, 1995) was used throughout this manuscript for GPCR transmembrane (TM) helices, while a recently proposed numbering scheme (de Graaf et al., 2008) was used to number the residues in the second extracellular loop (EL2). For explicitly numbering EL2 residues in specific receptors, the UniProt residue number is given as superscript after the EL2 number (e.g. F45.55¹⁶⁹ in human H₄R).

Construction H₄R models. First, a preliminary high-throughput receptor model of only the 7 TM helices H₄R was generated using the GPCRgen program (Bissantz et al., 2004) based on the high resolution carazolol bound crystal structure template of the adrenergic beta-2 receptor (Cherezov et al., 2007). The amino acid sequence alignments used for constructing the receptor models are shown in the Supplementary Figure I. This preliminary H₄R model was minimized with AMBER 10 (ambermd.org) using the AMBER03 force field (Wang et

MOL #63040

al., 2004) to relax the structure and remove steric bumps. The minimizations were performed by 1,000 steps of steepest descent followed by conjugate gradient until the root mean square gradient of the potential energy was lower than 0.05 kcal/mol. Å. A twin cut-off (12.0, 15.0 Å) was used to calculate non-bonded electrostatic interactions and the non-bonded pair-list was updated every 25 steps. Histamine was docked into this structure using '2-times speed-up' settings of Goldv4.0 (Verdonk et al., 2003). Experimentally-driven receptor-ligand H-bond constraints were used to guide the docking process in the receptor: 1) Between the protonated amine nitrogen atom of histamine and one of the carboxylate oxygen atoms (OD1) of D3.32; 2) between the τ nitrogen of the imidazole group of histamine and one of the carboxylate oxygen atoms of E5.46. Fifteen histamine poses were generated. The histamine-H₄R complex was minimized with AMBER 10 using the same settings as described above, including the same H-bond (hydrogen-acceptor distance and donor-hydrogen-acceptor angle) constraints restraints as used for docking with addition H-bond constraints between: 3) the sulphur atom of C3.36 and one of the carboxylate oxygens (OD2) of D3.32, in line with an earlier experimentally supported histamine-bound model of H₁R (Jongejan et al., 2005); 4) the amide nitrogen atom of the Q7.42 sidechain and one of the carboxylate oxygen atoms (OD2) of D3.32 in line with an earlier histamine-bound H₄R model (Jongejan et al., 2008). This minimized complex was refined by a second AMBER energy minimization without distance restraints. Histamine force-field parameters were derived using the Antechamber program (Wang et al., 2004) and partial charges for the substrates were derived using the AM1-BCC procedure in Antechamber. The second extracellular loop (EL2) was constructed using two subsequent Modeller 9v1 (Sali and Blundell, 1993) runs with an explicit disulfide bridge constraint between C3.25 and C45.50 and including the histamine binding pose in the TM template as 'block' residue. In the first run, the ADRB2 crystal structure (PDB code 2RH1.pdb (Cherezov et al., 2007) was used to model the part upstream of EL2. Out of the 15

MOL #63040

generated models, the model with highest Modeller score and EL2 loop conformations properly accommodating the original histamine binding orientation in the original TM model were selected as input for a second Modeller run. In this second run, the EL2 segment downstream from C45.50 was constructed. One out of 15 models was selected based on the criteria described before. The H₄R-histamine H-bond constraints earlier used for energy minimization were transformed into explicit upper-bound (3.5 Å) distance constraints in the Modeller runs. After optimization of the EL2 conformation, extracellular loops 1 and 3, intracellular loops 1 and 2, and helix 8 were constructed based on the ADRB2 crystal structure (Cherezov et al., 2007) using Modeller 9v1. Intracellular loop 3, and the N- and C-termini were not modelled. The amino acid sequence alignments used for constructing the receptor models are shown in Supplementary Figure I. The final receptor model was energy minimized with the initially minimized histamine docking pose as described before.

Clozapine and JNJ 7777120 were docked into this model using the following experimentally guided (Jongejan et al., 2008; Shin et al., 2002) H-bond constraints: 1) Between the protonated piperidine nitrogen atom of the ligand and one of the carboxylate oxygen atoms (OD1) of D3.32; 2) between the carboxamide (JNJ 7777120) or tricyclic ring (clozapine) nitrogen atom of the ligand and one of the carboxylate oxygen atoms of E5.46. In the JNJ 7777120-H₄R complex, the Chi₁ torsional angle of C3.36 was manually rotated from its g- to its t rotamer to mimic the inactive state of the receptor (Jongejan et al., 2005). The models of human H₄R L5.39V, N4.57H, and N4.57H/S5.43L mutants were built by mutating the corresponding residues of the wild-type ligand bound H₄R model using the “mutate” function of MOE 2008.10 (www.chemcomp.com). The resulting wild-type and mutant receptor-ligand models, including the docked ligands, were further minimized as described above.

RESULTS

Expression of H₄R orthologs. We comprehensively analyzed the ligand binding properties of the different H₄R species variants. Transient transfection of HEK 293T cells with cDNAs of the different H₄R orthologs resulted in an adequate expression of functional H₄R proteins (B_{\max} values: 1 - 6.9 pmol/mg protein, Supplementary Figure II), as estimated by the binding of the agonist radioligand [³H]histamine with nM affinities. The K_D values of [³H]histamine for the human, monkey, pig, guinea pig, dog, mouse, and rat H₄R are 9, 15, 11, 11, 75, 78, and 134 nM (Supplementary Figure II), respectively. These values indicate species differences up to 10-fold in binding the endogenous agonist, and are in agreement with values reported previously (Liu et al., 2001b; Oda et al., 2002; Oda et al., 2005; Oda et al., 2000). It should be noticed that differences in expression host as well as methodology may lead to variability in measured pharmacological values. Inter-species ligand affinity *ratios* determined with individual experimental setups are however consistent. The K_D value of [³H]histamine is four-fold higher for dog H₄R expressed in HEK 293T cells (current study) than for dog H₄R expressed in COS-7 cells (Jiang et al., 2008), while K_D values for human H₄R expressed in HEK 293T (Oda et al., 2000) is three-fold higher for human H₄R expressed in SK-N-MC cells (Liu et al., 2001). Furthermore, the K_i values of other H₄R ligands, such as 4-methylhistamine and thioperamide, for the dog H₄R from this study in HEK 293T cells are about five-fold higher than those reported previously in COS-7 cells (Jiang et al., 2008), whereas JNJ 7777120 affinity is in good agreement in both reports.

We showed that the binding of [³H]histamine is not affected by the presence of GTP or GTP γ S (Supplementary Figure III), indicating that the binding of histamine is independent of the G-protein coupling state of the receptor, as proposed earlier by Schneider et al. (Schneider et al., 2009). This, therefore, implies that the affinities of tested H₄R ligands determined by [³H]histamine displacement are independent of G-protein coupling-state of the

MOL #63040

receptors. We also observed that all of these H₄R orthologs are able to dose-dependently respond to histamine in a G α_{q15} /NFAT-luciferase reporter gene assay performed according to previously described methodology (Lim et al., 2008; Supplementary Figure IV). As described earlier (Lim et al., 2008; Liu et al., 2001b) and in line with the binding studies (Table 1), histamine was less potent at rat and mouse H₄R_s (Supplementary Table II).

Ligand binding affinity for H₄R orthologs.

Histamine binds the different H₄R orthologs, as described above, with affinities that vary up to 10-fold (Table 1 and Supplementary Figure II). As can be seen in Figure 2 and Table 1, also other H₄R ligands interact with the different species orthologs with varying affinities. The H₄R agonist 4-methylhistamine (Lim et al., 2005) consistently shows a slightly lower affinity than histamine for each of the orthologs, and the binding affinity of 4-methylhistamine shows the same trend as histamine for the various species variants (Table 1). The H₄R affinity of VUF 8430, a potent human H₄R agonist (Lim et al., 2006), does not completely follow this trend. Like histamine, VUF 8430 shows high affinity for human (pK_i 7.5) and monkey (pK_i 7.3) H₄R_s, but for the H₄R_s of the other species evaluated, the pK_i values of VUF 8430 is between 5.9 (dog) and 6.8 (rat) (Table 2, Figure 2).

Interestingly, the affinity of the non-imidazole H₄R agonist clozapine spans almost 3 log units across the tested H₄R orthologs, with the order of increasing affinity (in pK_i value): dog (4.5), pig (5.2), mouse (5.5), rat (5.6), human (6.4), monkey (7.3), and guinea pig (7.3) (Table 1, Figure 3). This large difference in affinity is also shown by other tested non-imidazole H₄R ligands, like JNJ 7777120 (Figure 2, Table 1) and its benzimidazole analog VUF 6002. Compared to JNJ 7777120, VUF 6002 consistently shows a 10-fold lower affinity for binding to the various orthologs, with the exception of the guinea pig H₄R, which binds JNJ 7777120 and VUF 6002 with equal affinity (Table 1).

The H₄R agonist/H₃R inverse agonist clobenpropit shows equipotent affinity for H₄R_s of human, monkey, mouse, and rat (pK_i values of 7.5, 7.5, 7.3, and 7.3, respectively), lower affinity for H₄R_s of pig and dog (pK_i values of 6.6 and 6.4, respectively), and an higher affinity for the guinea pig H₄R (pK_i value of 8.2) (Table 1). The K_i values for the human, mouse, and rat H₄R_s (stably expressed in HEK 293T cells) in this study are higher than those reported previously using H₄R_s expressed in SK-N-MC cells (Lim et al., 2003; Liu et al., 2002b). Finally, we observed that the H₄R inverse agonist thioperamide binds equipotently to all of the H₄R orthologs (pK_i values between 7.0 and 7.6), except for the dog H₄R which binds thioperamide with a lower pK_i of 6.4 (Figure 2, Table 1).

Residues involved in ligand binding affinity differences between human, rat and mouse H₄R have already been analyzed in earlier studies (Lim et al., 2008; Liu et al., 2001b). We therefore focused on the identification of key residues responsible for ligand binding affinity differences between human, pig, dog, and monkey H₄R orthologs.

Chimeric human-pig H₄R approach. The human and pig H₄R_s show equipotent affinity for histamine, but different affinity for clozapine, JNJ 7777120, and VUF 8430 (Table 1). These four ligands were therefore used in further studies to probe human-pig H₄R chimeras and pig H₄R-mimicking site-directed mutants of human H₄R. Based on our previous study on the pharmacological differences of the human and mouse H₄R_s, we employed a chimeric receptor approach to investigate the differences in binding profiles between the pig and human H₄R_s (Figure 3). The chimeric HPH (after human-pig-human) receptor expressed in HEK 293T cells (B_{max} = 2.9 pmol/mg protein) exhibits a K_D value of 18 nM for [³H]histamine (Table 2). Whereas the affinity of histamine for the HPH chimeric receptor is conserved, HPH shows significantly lower affinity for clozapine, JNJ 7777120, and VUF 8430 with pK_i values of 4.7, 6.1, and 6.3, respectively (Table 2, Figure 4), in comparison to the human H₄R. Expression of

MOL #63040

PHP (after pig-human-pig) chimeric receptor is significantly lower yet measurable ($B_{\max} = 0.3$ pmol/mg protein). The affinity of clozapine, JNJ 7777120, and VUF 8430 (pK_i values of 6.8, 7.8, and 7.4, respectively) for the PHP chimera is significantly increased compared to pig H_4R , mimicking the affinity profile of human H_4R (Table 2, Figure 4). These data clearly show that the middle H_4R domain (Table 2) is playing a crucial role in the binding of clozapine, JNJ 7777120 and VUF 8430.

Site-directed mutagenesis of the human H_4R . Following the results of the chimeric approach, we decided to continue with a site-directed mutagenesis (SDM) approach to further pinpoint the amino acid residues involved in the binding of clozapine, JNJ 7777120 and VUF 8430. The human and pig H_4R species variants show a total of 16 divergent amino acid residues in the middle domain of the HPH and PHP chimeras (Figure 3, shaded areas). Four divergent amino acids are located in the second intracellular loop or cytoplasmic half of TM4 (Figure 3), and were omitted for further analysis, since this domain is not likely to be involved in ligand binding to bioaminergic GPCRs (Shi and Javitch, 2002). We also excluded from our analysis the highly divergent stretch of four, six or ten amino acid residues in the second extracellular loop (DEGSE in the human H_4R and QGKQD in the pig H_4R , Figure 3), since our previous study did not implicate this region in ligand binding to human or mouse H_4Rs (Lim et al., 2008). All other amino acid residues that differ between human and pig H_4Rs were investigated for their involvement in ligand binding by constructing the human H_4R mutants N4.57H, M4.60V, S45.42¹⁵⁶A, F45.55¹⁶⁹L, F45.55¹⁶⁹L/S45.56¹⁷⁰K, I5.38V, S5.43L, and L5.45F. After expression in HEK 293T cells all mutant receptors still bound [³H]histamine with nM affinity (6-51 nM, Supplementary Table I) and were well expressed, with the exception of the human H_4R (h H_4R) mutant S45.42¹⁵⁶A, which showed high affinity for H_4R , but had very low expression (Supplementary Table I). The M4.60V, S45.42¹⁵⁶A,

MOL #63040

I5.38V, S5.43L, and L5.45F mutants of hH₄R did not show the change in pharmacology as observed in the HPH chimeric H₄R (Supplementary Table I). Only the S5.43L mutation resulted in a slight, but significant, 3-fold loss of the affinity of JNJ 7777120, but this mutation did not affect the affinities of histamine, clozapine or VUF 8430 (Supplementary Table I). In line with our previous work, showing the importance of the FF motif in EL2 for the binding of clozapine (Lim et al., 2008), both the F169^{45.55}L and the double mutant F169^{45.55}L/S170^{45.56}K show reduced affinity for clozapine (Supplementary Table I). However, the binding of none of the other ligands was altered upon the F169^{45.55}L and F169^{45.55}L/S170^{45.56}K mutations (Supplementary Table I).

The role of position 45.55 in ligand binding to H₄R has already been described in an earlier study (Lim et al., 2008). Table 2 presents three newly identified residues found to be responsible for ligand binding affinity differences between human, pig, dog, and monkey H₄R orthologs (N/H4.56, S/L5.43, and L/V5.39). The full list of investigated mutants is presented in Supplementary Table I. The human, monkey, guinea pig, pig, rat, and mouse H₄R contain at position 4.57 an asparagine residue, whereas the pig and dog H₄R possess a histidine residue at this position (Figure 4). While pig and human H₄R bind [³H]histamine with high affinity (K_D values of 9 and 11 nM, respectively, see Table 2), dog H₄R and the N4.57H hH₄R mutant bind [³H]histamine with low affinity (K_D values of 75 and 51 nM, respectively). The N4.57H hH₄R mutant mimicks the pig and dog H₄R and binds clozapine, VUF 8430 and JNJ 7777120 with significantly lower affinity than wild-type hH₄R (Table 2, Figure 4). The affinities of the agonists clozapine and VUF 8430 for this mutant are similar to the affinities observed for the HPH chimeric H₄R protein, but the affinity of the H₄R antagonist JNJ 7777120 is only partially reduced by the N4.57H mutation (Table 2, Figure 4). Apparently, other residues within the swapped region of the HPH chimeric receptor contribute to the difference in pharmacology between human and pig H₄R as well. Interestingly, pig differs

MOL #63040

from human and dog H₄R at position 5.43 (a serine instead of a leucine residue, Figure 3), and we hypothesized that this residue might compensate for the negative effect of the N4.57H mutation on histamine binding, while further decreasing binding affinity for JNJ 7777120. We therefore constructed the N4.57H/S5.42L hH₄R double mutant, increasing the resemblance with the binding pocket of the pig H₄R (Figure 3). Interestingly, the double hH₄R mutant N4.57H/S5.43L showed the predicted increase in affinity for [³H]histamine (Table 2). The double mutant does not show full conversion to the pharmacological profile of pig H₄R, as the affinity for JNJ 7777120 is only slightly further decreased in the double mutant compared to the N4.57H and/or S5.43 single mutants (Table 2).

The monkey and human H₄R have a high sequence homology (91%, Figure 1)), but they show significantly different affinity for JNJ 7777120 and clozapine (Table 1). Compared to the human H₄R, the monkey H₄R shows a 10-fold higher affinity for clozapine (pK_i = 7.3 v.s. 6.4), but shows an almost 10-fold lower affinity for JNJ 7777120 (pK_i = 7.5 v.s. 8.3). We exploited the small differences in protein sequence between the monkey and human H₄R to study ligand-H₄R interactions. In the extracellular domains, two residues within EL3 and one within EL2 differ (Figure 5). Our previous study on the difference between human and mouse H₄R indicated that these residues are not involved in ligand binding (Lim et al., 2008), and thus they were not included in our SDM approach. Within the transmembrane domains only 6 amino acids differ between the human and the monkey receptor protein (Figure 5). Four divergent amino acids are located in TM1 and TM2, which are usually not part of the main ligand binding pocket of bioaminergic GPCRs (Shi and Javitch, 2002). Two other residues are located in TM5; the human H₄R has a Val residue at position 5.48, whereas a Leu residue is present in the monkey H₄R and the other species orthologs, including the mouse and rat H₄R (Jiang et al., 2008). Since JNJ 7777120 shows equipotent affinity for the human, mouse and rat H₄R, we argued that the difference of residue 5.48 is unlikely to be responsible for the

MOL #63040

difference in JNJ 7777120 affinity between monkey and human H₄Rs. Residue 5.39 is valine in the monkey or leucine in the human, mouse, and rat H₄Rs. We therefore selected this residue as the prime cause for the difference in affinity of JNJ 7777120 between the human and monkey H₄Rs. The human H₄R mutant L5.39V was constructed and expressed in HEK 293T cells. Compared to the wild type human H₄R, the H₄R L5.39V mutant shows a low affinity for JNJ 7777120, like the monkey H₄R (Table 2, Figure 6). Moreover, clozapine shows an increase in affinity at the H₄R L5.39V mutant and binds the mutant H₄R like the monkey H₄R (Table 2, Figure 6).

MOL #63040

DISCUSSION

Significant differences in ligand binding affinity between H₄R orthologs. In order to understand the action of newly developed H₄R ligands in translational preclinical studies in animal models of disease, we comprehensively characterized the binding of selected H₄R ligands on heterologously expressed H₄R species variants in HEK 293T cells, including those of human, monkey, pig, dog, mouse, rat, and guinea pig. Important results from our studies are the identification of substantial compound-specific pharmacology across the various H₄R proteins, suggesting potential problems in the interpretation of in vivo results in animal models. The H₄R proteins of human, monkey, pig, and guinea pig bind histamine with high affinity, while those of dog, mouse, and rat interact with the agonist with lower affinity (Table 1 and Supplementary Figure II). Interestingly, the high histamine affinity for the H₄R_s expressed in HEK 293T cells are not affected by G-protein uncoupling reagents, such as GTP or GTP γ S (Supplementary Figure III). Indeed, the H₄R alone shows a high affinity for the agonist histamine in Sf9 cells, which is lacking G-proteins that are able to couple to H₄R (Schneider et al., 2009). Moreover, neither co-expression or fusion of G α_{i2} changes the histamine affinity for H₄R, which suggest the existence of a G-protein-independent high-affinity receptor state of H₄R (Schneider, et al., 2009).

4-Methylhistamine shows the same trend in binding affinity for H₄R orthologs as histamine (Table 1) (Lim et al., 2005), albeit with slightly lower affinity. The recently discovered H₄R agonist, VUF 8430 (Lim et al., 2006), does not follow the trend of histamine affinity for the orthologs. The tricyclic H₄R agonist clozapine shows large difference in affinity for the H₄R orthologs. In comparison to the affinity for the human H₄R, a significant drop in affinity is observed for the pig, dog, mouse, and rat H₄R_s (Table 1). Monkey and guinea pig H₄R_s, on the contrary, show higher affinity for clozapine. Importantly, JNJ 7777120 and VUF 6002, two H₄R antagonists that have been used in several in vivo H₄R

MOL #63040

studies, show significantly lower affinity for monkey, pig, dog, and guinea pig H₄Rs (Table 1). The interspecies differences in ligand affinity have limited their use and these H₄R antagonists have to be used with caution for experiments in the indicated animals. In contrast, thioperamide shows an equipotent affinity for the species variants and consistently acts as an antagonist or inverse agonist at these species variants (Lim et al., unpublished data). Therefore, despite its cross reactivity at the H₃R, thioperamide might be used as H₄R antagonists in the species variants that show low affinity for JNJ 777120.

Using chimeric human-pig-human and pig-human-pig H₄R proteins and SDM studies, we have systematically identified residues at positions 45.55 (in EL2), 4.57, 5.39, and S5.43 as residues responsible for the observed species differences (Table 2 and Supplementary Table I). While the role of position 45.55 in ligand binding to H₄R has already been described in an earlier study (Lim et al., 2008), we will discuss the role of the other three residues in more detail in the following paragraphs.

H4.57 negatively affects ligand binding in pig and dog H₄Rs. SDM studies have identified the residue at position 4.57 (Asn in human, mouse, rat, monkey, and guinea pig, His in dog and pig) as an amino acid responsible for differences in ligand affinity for H₄R orthologs (Table 2). While earlier SDM studies already showed the importance of N4.57 in histamine-induced H₄R activation (Shin et al., 2002), our current studies show that clozapine affinity is largely decreased in the human H₄R N4.57H mutant (Table 2). The effect of this mutation on histamine, JNJ 777120 and VUF 8430 affinity is less dramatic, but still significant (Table 2). Interestingly, the high affinity for histamine is recovered in the pig mimicking N4.57H/S5.43L double mutant. The subtle roles of N4.57H and S5.43L in histamine binding are rationalized by our H₄R modeling studies as demonstrated in Figure 7A-B. The protonated amine group of histamine forms a complementary H-bond network with D3.32, C3.36, and

MOL #63040

Q7.42, while the histamine imidazole group stacks between Y3.33 and Y6.51, and donates an H-bond to E5.46 (Figure 7A). This binding mode is in line with earlier SDM studies indicating the essential role of D3.32 and E5.46 in histamine binding in H₄R (Jongejan et al., 2008; Shin et al., 2002), and the experimentally supported role of the homologous S3.36 residue in H₁R (Jongejan et al., 2005). In wild-type H₄R, N4.57 donates H-bonds to the backbone carbonyl atom of A4.53 and the hydroxyl group of T3.37. An alternative H-bond network is formed in the pig and dog mimicking N4.57H mutant in which the histidine residue is able to donate an H-bond to the carboxylate group E5.46, which in its turn also accepts an H-bond from T3.37. This H-bond network reorients E5.46 more towards TM4. To maintain the essential H-bond with E5.46 (Jongejan et al., 2008), histamine has to reorient its imidazole ring deeper into the binding pocket. This alternative binding pose is stabilized by the leucine side chain in the S5.43L/N4.57H mutant (Figure 7B), explaining the increased binding affinity for histamine in this pig mimicking double mutant over the dog mimicking N4.57H single mutant (Table 2). The full agonist clozapine forms an H-bond between its positively charged piperidine nitrogen atom and the carboxylate group of D3.32 in the pocket between TMs 2, 3, and 7 (subpocket i) and forces C3.36 in its g- conformation (which has been associated with the activated state of H₁R (Jongejan et al., 2005)) by placing its chlorinated aromatic ring in the hydrophobic binding pocket between TMs 3, 4, 5, and 6 (subpocket ii) (Figs. 7C and 8A). The non-chlorinated aromatic ring stacks between Y3.33 and Y6.51, while the nitrogen atom in the tricyclic ring system donates an H-bond to E5.46 (Figure 8A). This binding mode is in line with the selectivity profile of clozapine and olanzapine for bioaminergic receptor subtypes (Selent et al., 2008) and structure-activity relationship studies of clozapine analogues indicating the steric restriction around the tricyclic nitrogen atom and the importance of 7- and 8-substitution over 2- and 3- substitution (Smits et al., 2006). The reorientation of E5.46 in the pig and dog mimicking N4.57H mutant towards

MOL #63040

TM4 disrupts the H-bond with the NH group of clozapine as its rigid cyclic ring is tightly bound in subpocket ii (Figure 7C), explaining the large decrease in clozapine binding affinity at the N4.57H mutant as well as at pig and dog H₄Rs.

Residue 5.39 distinguishes the human and monkey H₄Rs. Despite the high homology between these two orthologs (93%), significant differences exist for the binding of clozapine and JNJ 7777120. Our SDM studies identified residue 5.39 as the cause of the pharmacological differences between the human and monkey H₄R. In H₁R, K5.39 is known to interact with histamine and zwitterionic H₁R antagonists (Gillard et al., 2002; Leurs et al., 1995). In human H₄R, the full agonist clozapine is positively affected by the L5.39V mutation. The valine residue in the monkey H₄R mimicking L5.39V mutant is sterically limited because of a steric clash with the helical backbone (Lovell et al., 2000) and forms a complementary cap with its CG2 methyl group on top of the non-chlorinated aromatic ring of clozapine (Figure 8A). The leucine residue in wild-type human H₄R on the other hand, is more flexible and can orient its iso-butyl side chain in a *trans* conformation (Lovell et al., 2000) pointing outwards of the binding pocket, explaining the gain of affinity in the L5.39V mutant. The antagonist JNJ 7777120 forms an ionic/H-bond between its positively charged piperazine nitrogen atom and D3.32, but stabilizes C3.36 in its inactive (Jongejan et al., 2005) *trans* conformation by accepting an H-bond with its piperazine carbonyl oxygen and donating an H-bond from its indole nitrogen to the carboxylate group of E5.46. The chlorinated aromatic ring is stacked between Y3.33 and Y6.51 and occupies a pocket between TMs 3, 5, 6, and EL2 (Figure 8B). Previous SDM studies have shown the importance of D3.32 as well as E5.46 as critical ionic interaction point and H-bond acceptor, respectively (Jongejan et al., 2008), and are in line with the proposed JNJ 7777120 binding mode. Structure-activity relationships of JNJ 7777120 analogues, indicating the importance of the H-bond donor

MOL #63040

functionality of the indole nitrogen, the preference for 4- and 5-substitution over 6- and 7-substitution, and the toleration of polar groups at the 5-position of the aromatic ring (Jablonowski et al., 2003) support this binding pose instead of an orientation in which the chlorinated aromatic ring binds into the highly hydrophobic pocket close to W6.48 between TM3, 4, 5, and 6. The negative effect of the L5.39V mutation further supports the proposed binding mode. In the mutant, the CG2 methyl group of the sterically restricted valine residue bumps into the chlorine atom of JNJ 7777120, while the more flexible leucine residue in the wild-type can avoid this clash (Figure 8B).

CONCLUSIONS

In conclusion, we have pharmacologically characterized seven H₄R species orthologs that are relevant in drug discovery, i.e. human, monkey, pig, dog, mouse, rat, and guinea pig H₄R. We have described profound differences in the binding of an extensive set of reference H₄R ligands, providing important information for a good understanding of the action of these ligands in animal models of disease. The current work demonstrates the usefulness of the differences in amino acid sequence between the various species variants (natural mutagenesis) to study H₄R-ligand interactions. Domain swapping of the protein sequence of the human and pig H₄R enabled us to identify the middle domain of the H₄R as the cause of the observed species difference. SDM studies identified the residue at position 4.57 as an important determinant for the species difference in ligand affinity, while the difference between human and monkey H₄R in ligand binding can be explained by a single mutation of position 5.39. Structural models of wild-type and mutant human H₄R were used to explain the role of these critical residues in ligand binding. These results altogether improve our understanding of H₄R-ligand interactions and provide valuable information for the construction and refinement

MOL #63040

of structural models of H₄R-ligand complexes, which can eventually be used for structure-based H₄R virtual screening and ligand design.

ACKNOWLEDGMENTS

Saskia Nijmeijer is acknowledged for technical assistance with the functional assays.

MOL #63040

REFERENCES

- Ballesteros J and Weinstein H (1995) Integrated methods for the construction of three-dimensional models and computational probing of structure-function relations of G protein-coupled receptors. *Methods Neurosci* **25**:366-428.
- Bissantz C, Logean A and Rognan D (2004) High-throughput modeling of human G-protein coupled receptors: amino acid sequence alignment, three-dimensional model building, and receptor library screening. *J Chem Inf Comput Sci* **44**(3):1162-1176.
- Buckland KF, Williams TJ and Conroy DM (2003) Histamine induces cytoskeletal changes in human eosinophils via the H₄ receptor. *Br J Pharmacol* **140**(6):1117-1127.
- Celanire S, Wijtman M, Talaga P, Leurs R and de Esch IJ (2005) Keynote review: histamine H₃ receptor antagonists reach out for the clinic. *Drug Discov Today* **10**(23-24):1613-1627.
- Cherezov V, Rosenbaum DM, Hanson MA, Rasmussen SG, Thian FS, Kobilka TS, Choi HJ, Kuhn P, Weis WI, Kobilka BK and Stevens RC (2007) High-resolution crystal structure of an engineered human β 2-adrenergic G protein-coupled receptor. *Science* **318**(5854):1258-1265.
- de Graaf C, Foata N, Engkvist O and Rognan D (2008) Molecular modeling of the second extracellular loop of G-protein coupled receptors and its implication on structure-based virtual screening. *Proteins* **71**(2):599-620.
- Gillard M, Van Der Perren C, Moguilevsky N, Massingham R and Chatelain P (2002) Binding characteristics of cetirizine and levocetirizine to human H₁ histamine receptors: contribution of Lys(191) and Thr(194). *Mol Pharmacol* **61**(2):391-399.
- Hancock AA (2006) The challenge of drug discovery of a GPCR target: analysis of preclinical pharmacology of histamine H₃ antagonists/inverse agonists. *Biochem Pharmacol* **71**(8):1103-1113.
- Hough LB (2001) Genomics meets histamine receptors: new subtypes, new receptors. *Mol Pharmacol* **59**(3):415-419.
- Jablonowski JA, Grice CA, Chai W, Dvorak CA, Venable JD, Kwok AK, Ly KS, Wei J, Baker SM, Desai PJ, Jiang W, Wilson SJ, Thurmond RL, Karlsson L, Edwards JP, Lovenberg TW and Carruthers NI (2003) The first potent and selective non-imidazole human histamine H₄ receptor antagonists. *J Med Chem* **46**(19):3957-3960.
- Jiang W, Lim HD, Zhang M, Desai P, Dai H, Colling PM, Leurs R and Thurmond RL (2008) Cloning and pharmacological characterization of the dog histamine H₄ receptor. *Eur J Pharmacol*. **592** (1-3):26-32.
- Jongejan A, Bruysters M, Ballesteros JA, Haaksma E, Bakker RA, Pardo L and Leurs R (2005) Linking agonist binding to histamine H₁ receptor activation. *Nat Chem Biol* **1**(2):98-103.
- Jongejan A, Lim HD, Smits RA, de Esch IJ, Haaksma E and Leurs R (2008) Delineation of agonist binding to the human histamine H₄ receptor using mutational analysis, homology modeling, and ab initio calculations. *J Chem Inf Model* **48**(7):1455-1463.
- Leurs R, Smit MJ, Meeder R, Ter Laak AM and Timmerman H (1995) Lysine200 located in the fifth transmembrane domain of the histamine H₁ receptor interacts with histamine but not with all H₁ agonists. *Biochem Biophys Res Commun* **214**(1):110-117.
- Lim HD, Jongejan A, Bakker RA, Haaksma E, de Esch IJ and Leurs R (2008) Phenylalanine169 in the second extracellular loop of the human histamine H₄ receptor is responsible for the difference in agonist binding between human and mouse H₄ receptors. *J Pharmacol Exp Ther*. **327**(1):88-96.
- Lim HD, Smits RA, Bakker RA, van Dam CM, de Esch IJ and Leurs R (2006) Discovery of S-(2-guanidylethyl)-isothiourrea (VUF 8430) as a potent nonimidazole histamine H₄ receptor agonist. *J Med Chem* **49**(23):6650-6651.

MOL #63040

- Lim HD, van Rijn RM, Ling P, Bakker RA, Thurmond RL and Leurs R (2005) Evaluation of histamine H₁-, H₂-, and H₃-receptor ligands at the human histamine H₄ receptor: identification of 4-methylhistamine as the first potent and selective H₄ receptor agonist. *J Pharmacol Exp Ther* **314**(3):1310-1321.
- Liu C, Ma X, Jiang X, Wilson SJ, Hofstra CL, Blevitt J, Pyati J, Li X, Chai W, Carruthers N and Lovenberg TW (2001a) Cloning and pharmacological characterization of a fourth histamine receptor H₄ expressed in bone marrow. *Mol Pharmacol* **59**(3):420-426.
- Liu C, Wilson SJ, Kuei C and Lovenberg TW (2001b) Comparison of human, mouse, rat, and guinea pig histamine H₄ receptors reveals substantial pharmacological species variation. *J Pharmacol Exp Ther* **299**(1):121-130.
- Lovell SC, Word JM, Richardson JS and Richardson DC (2000) The penultimate rotamer library. *Proteins* **40**(3):389-408.
- Maconi A, Pastorin G, Da Ros T, Spalluto G, Gao ZG, Jacobson KA, Baraldi PG, Cacciari B, Varani K, Moro S and Borea PA (2002) Synthesis, biological properties, and molecular modeling investigation of the first potent, selective, and water-soluble human A₃ adenosine receptor antagonist. *J Med Chem* **45**(17):3579-3582.
- Oda T, Matsumoto S, Masuho Y, Takasaki J, Matsumoto M, Kamohara M, Saito T, Ohishi T, Soga T, Hiyama H, Matsushime H and Furuichi K (2002) cDNA cloning and characterization of porcine histamine H₄ receptor. *Biochim Biophys Acta* **1575**(1-3):135-138.
- Oda T, Matsumoto S, Matsumoto M, Takasaki J, Kamohara M, Soga T, Hiyama H, Kobori M and Katoh M (2005) Molecular cloning of monkey histamine H₄ receptor. *J Pharmacol Sci* **98**(3):319-322.
- Oda T, Morikawa N, Saito Y, Masuho Y and Matsumoto S (2000) Molecular cloning and characterization of a novel type of histamine receptor preferentially expressed in leukocytes. *The J Biol Chem* **275**(47):36781-36786.
- Oksenberg D, Marsters SA, O'Dowd BF, Jin H, Havlik S, Peroutka SJ and Ashkenazi A (1992) A single amino-acid difference confers major pharmacological variation between human and rodent 5-HT_{1B} receptors. *Nature* **360**(6400):161-163.
- Parsons ME and Ganellin CR (2006) Histamine and its receptors. *Br J Pharmacol* **147 Suppl 1**:S127-135.
- Reinhart GJ, Xie Q, Liu XJ, Zhu YF, Fan J, Chen C and Struthers RS (2004) Species selectivity of nonpeptide antagonists of the gonadotropin-releasing hormone receptor is determined by residues in extracellular loops II and III and the amino terminus. *J Biol Chem* **279**(33):34115-34122.
- Sali A and Blundell TL (1993) Comparative protein modelling by satisfaction of spatial restraints. *J Mol Biol* **234**(3):779-815.
- Schneider EH, Schnell D, Papa D, Seifert R (2009) High constitutive activity and a G-protein-independent high-affinity state of the human histamine H₄-receptor. *Biochemistry* **48**:1424-38.
- Selent J, Lopez L, Sanz F and Pastor M (2008) Multi-receptor binding profile of clozapine and olanzapine: a structural study based on the new beta2 adrenergic receptor template. *ChemMedChem* **3**(8):1194-1198.
- Shi L and Javitch JA (2002) The binding site of aminergic G protein-coupled receptors: the transmembrane segments and second extracellular loop. *Annu Rev Pharmacol Toxicol* **42**:437-467.
- Shin N, Coates E, Murgolo NJ, Morse KL, Bayne M, Strader CD and Monsma FJ, Jr. (2002) Molecular modeling and site-specific mutagenesis of the histamine-binding site of the histamine H₄ receptor. *Mol Pharmacol* **62**(1):38-47.

MOL #63040

- Smits RA, Leurs R and de Esch IJ (2009) Major advances in the discovery of histamine H₄ receptor ligands. *Drug Discov Today*. **14**(15-16):745-753.
- Smits RA, Lim HD, Stegink B, Bakker RA, de Esch IJ and Leurs R (2006) Characterization of the histamine H₄ receptor binding site. Part 1. Synthesis and pharmacological evaluation of dibenzodiazepine derivatives. *J Med Chem* **49**(15):4512-4516.
- Takeshita K, Sakai K, Bacon KB and Gantner F (2003) Critical role of histamine H₄ receptor in leukotriene B₄ production and mast cell-dependent neutrophil recruitment induced by zymosan in vivo. *J Pharmacol Exp Ther* **307**(3):1072-1078.
- Terzioglu N, van Rijn RM, Bakker RA, De Esch IJ and Leurs R (2004) Synthesis and structure-activity relationships of indole and benzimidazole piperazines as histamine H₄ receptor antagonists. *Bioorg Med Chem Lett* **14**(21):5251-5256.
- Thurmond RL, Desai PJ, Dunford PJ, Fung-Leung WP, Hofstra CL, Jiang W, Nguyen S, Riley JP, Sun S, Williams KN, Edwards JP and Karlsson L (2004) A potent and selective histamine H₄ receptor antagonist with anti-inflammatory properties. *J Pharmacol Exp Ther* **309**(1):404-413.
- Thurmond RL, Gelfand EW and Dunford PJ (2008) The role of histamine H₁ and H₄ receptors in allergic inflammation: the search for new antihistamines. *Nat Rev Drug Discov* **7**(1):41-53.
- Venable JD, Cai H, Chai W, Dvorak CA, Grice CA, Jablonowski JA, Shah CR, Kwok AK, Ly KS, Pio B, Wei J, Desai PJ, Jiang W, Nguyen S, Ling P, Wilson SJ, Dunford PJ, Thurmond RL, Lovenberg TW, Karlsson L, Carruthers NI and Edwards JP (2005) Preparation and biological evaluation of indole, benzimidazole, and thienopyrrole piperazine carboxamides: potent human histamine H₄ antagonists. *J Med Chem* **48**(26):8289-8298.
- Verdonk ML, Cole JC, Hartshorn MJ, Murray CW and Taylor RD (2003) Improved protein-ligand docking using GOLD. *Proteins* **52**(4):609-623.
- Wang J, Wolf RM, Caldwell JW, Kollman PA and Case DA (2004) Development and testing of a general amber force field. *J Comput Chem* **25**(9):1157-1174.

MOL #63040

FOOTNOTES

This work was supported by the Top Institute Pharma [project number D1.105: the GPCR Forum] and COST Action BM0806.

*These authors equally contributed to the work

¹Current affiliation: Boehringer Ingelheim Pharma GmbH and Co. KG, Biberach, Germany.

For reprint request:

Prof. Dr. Rob Leurs

Leiden/Amsterdam Center for Drug Research, Division of Medicinal Chemistry, Faculty of Science, VU University Amsterdam

De Boelelaan 1083

1081 HV Amsterdam, The Netherlands.

E-mail: r.leurs@few.vu.nl

MOL #63040

LEGENDS FOR FIGURES

Figure 1. Homology (%) of protein sequences of the histamine H₄R of human (hm), *M. fascicularis* monkey (mk), pig (pg), dog (dog), guinea pig (gp), rat (rt), and mouse (ms).

Figure 2. Displacement of [³H]histamine binding by H₄R ligands VUF 8430 (**A**), clozapine (**B**), JNJ 7777120 (**C**), and thioperamide (**D**) at the human, monkey, pig, and dog H₄R. The error bars indicate the standard error of mean (SEM) of results of at least three independent experiments.

Figure 3. Alignment of the partial sequences (from residue D3.49 to F5.47 according to the Ballesteros-Weinstein numbering system) of various species variants of the H₄R. The residues that differ between the human and pig H₄R are shaded, and the human H₄R residues that are mutated into the pig/dog or maccaca H₄R counterparts are printed in bold and indicated by Ballesteros-Weinstein number. The FF-motif in EL2 is in *italics*. The domains of HPH and PHP chimeric receptors were swapped at the indicated *Cla*I and *Eco*RI restriction sites in the cDNAs of the human and pig H₄R.

Figure 4. Displacement of [³H]histamine binding by clozapine (**A**) and VUF 8430 (**B**) at the human H₄R, pig H₄R, chimeric HPH H₄R, and human H₄R N4.57H mutant expressed in HEK 293T cells. The error bars indicate the standard error of mean (SEM) of results of at least three independent experiments.

Figure 5. Snake plot of the monkey H₄R. The residues indicated in black differ between the monkey and human H₄R.

Figure 6. Displacement of [^3H]histamine binding by JNJ 7777120 (**A**) and clozapine (**B**) at the human H_4R , monkey H_4R and human H_4R L5.39V mutant expressed in HEK 293T cells. The error bars indicate the standard error of mean (SEM) of results of at least three independent experiments.

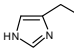
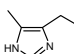
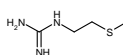
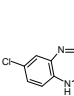
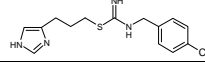
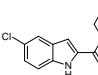
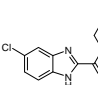
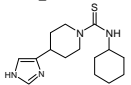
Figure 7. Binding modes of: (A) histamine (magenta carbon atoms, see Table 2 for 2-D representation) in the wild-type human H_4R receptor model, (B) histamine in the N4.57H/S5.43L double mutant, and (C) clozapine in the N4.57H single mutant. The backbone of TM helices 4, 5, 6, and 7 are represented by yellow ribbons and part of TM3 is shown as ribbon (the top of the helix is not shown for clarity). Important binding residues are depicted as ball-and-sticks with grey carbon atoms. The carbon atoms of mutated residues are coloured green. Oxygen, nitrogen sulphur, chlorine, and hydrogen atoms are coloured red, blue, orange, brown, and cyan, respectively. H-bonds described in the text are depicted by black dotted lines.

Figure 8. Binding modes of: (A) clozapine (magenta carbon atoms, see Table 2 for 2-D representation) and (B) JNJ 7777120 in wild-type/L5.39V mutant human H_4R receptor models. Rendering and colour coding is the same as in Figure 8. The sidechain atoms of L5.39 and V5.39 are depicted by grey and green ball and sticks, while the CG2 methyl group of V5.39 is additionally shown as semi-transparent green Van der Waals spheres. Numbers of different positions on the aromatic rings of clozapine and JNJ 7777120 are discussed in the text. The C3 methyl group of clozapine and the 5-chlorine atom of JNJ 7777120 are depicted by semi-transparent magenta and brown Van der Waals spheres, respectively.

MOL #63040

TABLES

Table 1. Affinity (pK_i) of H₄R ligands for different H₄R species variants. The data are presented as mean ± S.E.M. of at least three independent experiments.

Ligand	pK _i at H ₄ R species variant						
	human	monkey	Pig	dog	mouse	rat	guinea pig
Histamine 	7.9±0.1	7.8±0.1	7.9±0.1	7.2±0.1	7.1±0.1	7.0±0.1	8.0±0.1
4-MeHA 	7.3±0.1	7.0±0.1	7.7±0.1	6.3±0.1	6.8±0.1	6.4±0.1	7.3±0.1
VUF 8430 	7.5±0.1	7.3±0.1	6.5±0.1	5.9±0.1	6.7±0.1	6.8±0.1	6.3±0.1
Clozapine 	6.4±0.1	7.3±0.1	5.2±0.1	4.5±0.1	5.5±0.1	5.6±0.2	7.3±0.1
Clobenpropit 	7.5±0.1	7.5±0.1	6.6±0.1	6.5±0.1	7.3±0.1	7.3±0.1	8.2±0.1
JNJ 7777120 	8.3±0.1	7.5±0.1	6.3±0.1	7.1±0.1	8.4±0.1	8.4±0.1	6.0±0.1
VUF 6002 	7.5±0.1	6.7±0.1	5.1±0.1	6.2±0.1	6.9±0.1	7.3±0.1	5.8±0.1
Thioperamide 	7.1±0.1	7.1±0.1	7.0±0.1	6.4±0.1	7.6±0.1	7.5±0.1	7.1±0.1

MOL #63040

Table 2. Affinity (pK_i) of H₄R ligands at the human, pig, and dog H₄R_s and selected human H₄R mutants. Equilibrium dissociation constants (K_D) and B_{max} values for [³H]histamine (pmol/mg protein) and pK_i of H₄R ligands are presented as average \pm standard error of mean (SEM) of results of at least three independent experiments. The full list of investigated mutants is presented in Supplementary Table I.

Receptor	[³ H]histamine		pK_i			
	K_D (nM)	B_{max}	Histamine	Clozapine	JNJ 7777120	VUF 8430
Human H ₄ R	9 \pm 1	3.1 \pm 1.1	7.9 \pm 0.1	6.4 \pm 0.1	8.3 \pm 0.1	7.5 \pm 0.1
Pig H ₄ R	11 \pm 3	1.0 \pm 0.3	7.8 \pm 0.1	5.2 \pm 0.1	6.3 \pm 0.1	6.5 \pm 0.1
PHP chimera	4 \pm 1	0.3 \pm 0.1	8.3 \pm 0.1	6.8 \pm 0.1	7.8 \pm 0.1	7.4 \pm 0.1
HPH chimera	18 \pm 2	2.9 \pm 0.2	7.8 \pm 0.1	4.7 \pm 0.1	6.1 \pm 0.1	6.3 \pm 0.2
N4.57H/S5.43L	15 \pm 3	1.9 \pm 0.3	7.8 \pm 0.1	4.9 \pm 0.1	7.5 \pm 0.1	6.5 \pm 0.1
Dog H ₄ R	75 \pm 14	3.7 \pm 0.8	6.9 \pm 0.1	4.5 \pm 0.1	7.1 \pm 0.1	5.9 \pm 0.1
N4.57H	51 \pm 5	2.2 \pm 0.5	7.4 \pm 0.1	4.7 \pm 0.1	7.7 \pm 0.1	6.8 \pm 0.1
mkH4R	15 \pm 2	6.9 \pm 0.7	7.8 \pm 0.1	7.2 \pm 0.1	7.4 \pm 0.1	7.3 \pm 0.1
L5.39V	10 \pm 3	3.5 \pm 0.6	8.0 \pm 0.1	7.0 \pm 0.1	7.1 \pm 0.1	n.t. ^a

^a) Not tested

Hm	100						
Mk	93	100					
Pg	70	70	100				
Dg	71	71	71	100			
Gp	62	64	61	61	100		
Rt	68	68	66	65	61	100	
Ms	67	66	65	66	62	85	100
	Hm	Mk	Pg	Dg	Gp	Rt	Ms

Figure 1

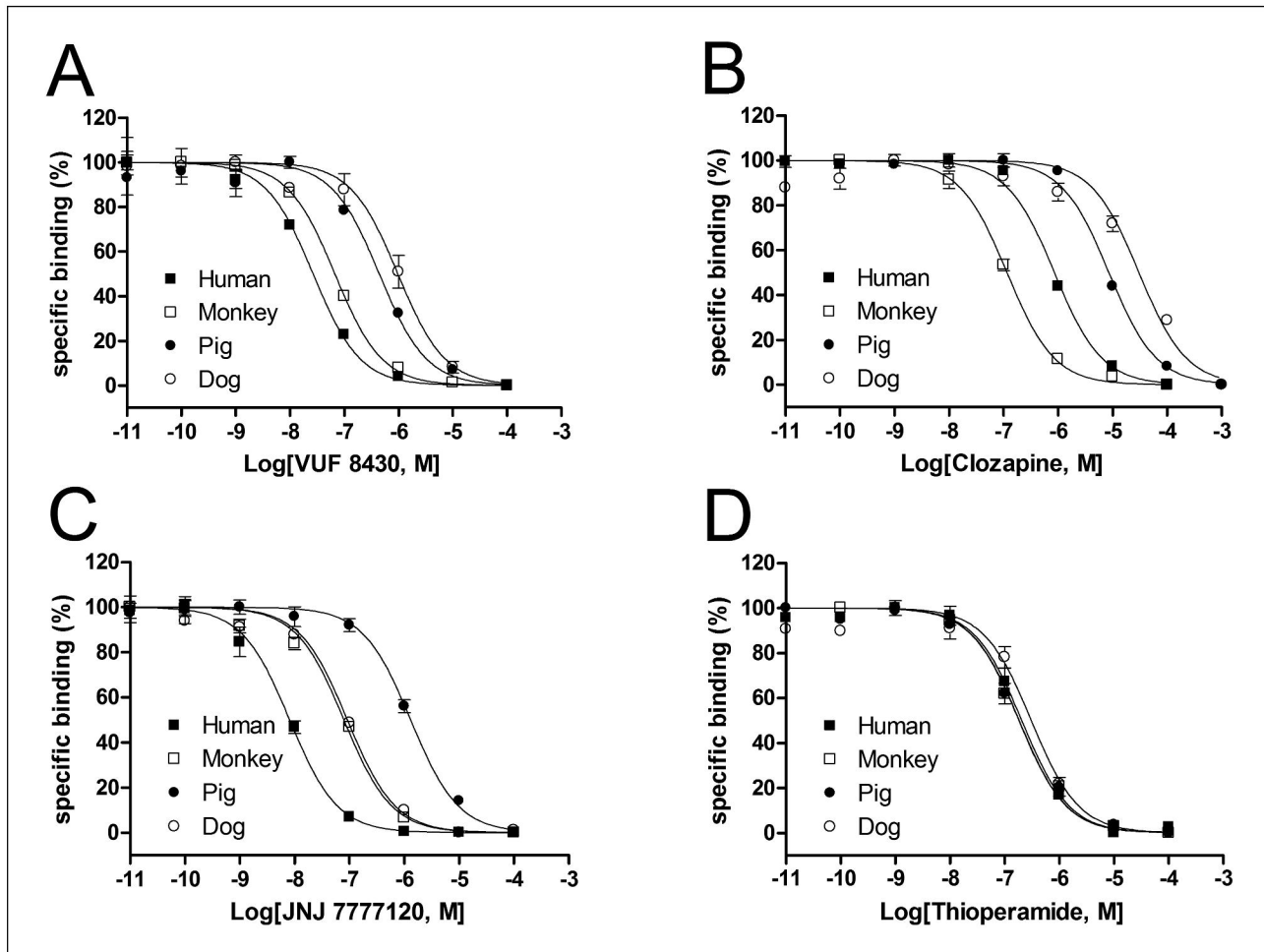


Figure 2

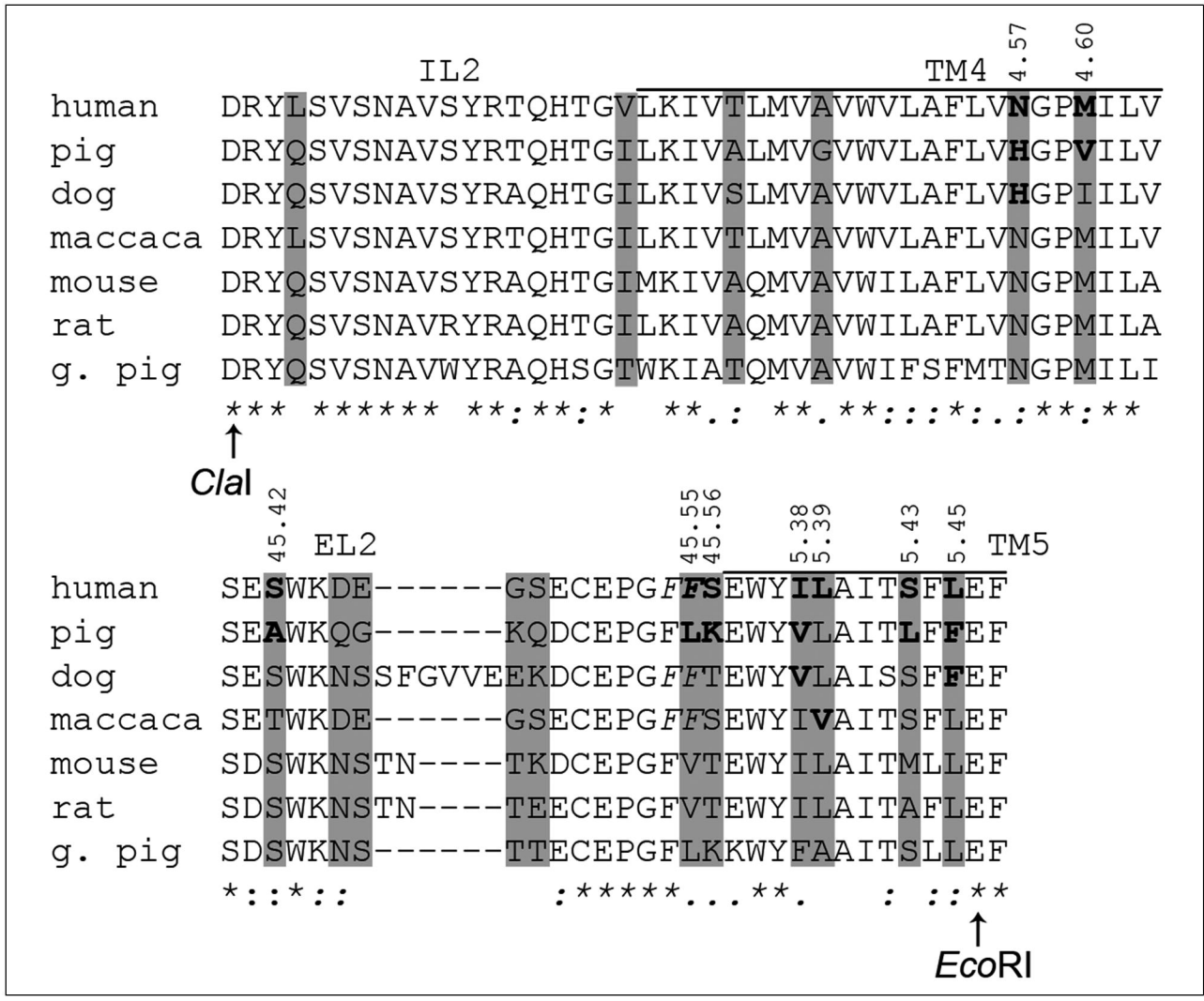


Figure 3

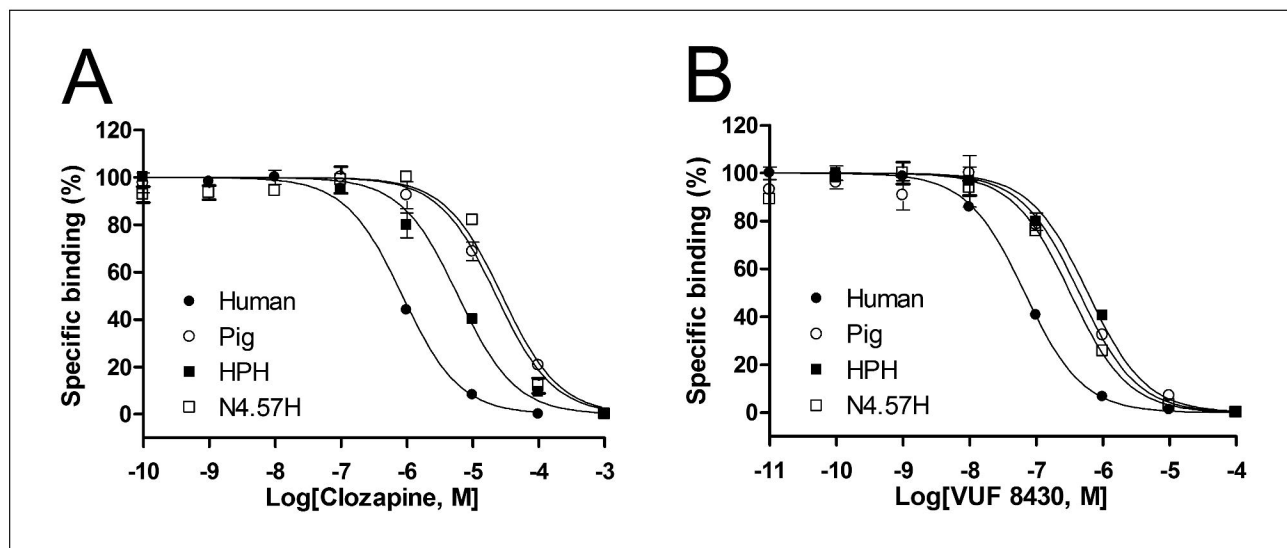


Figure 4

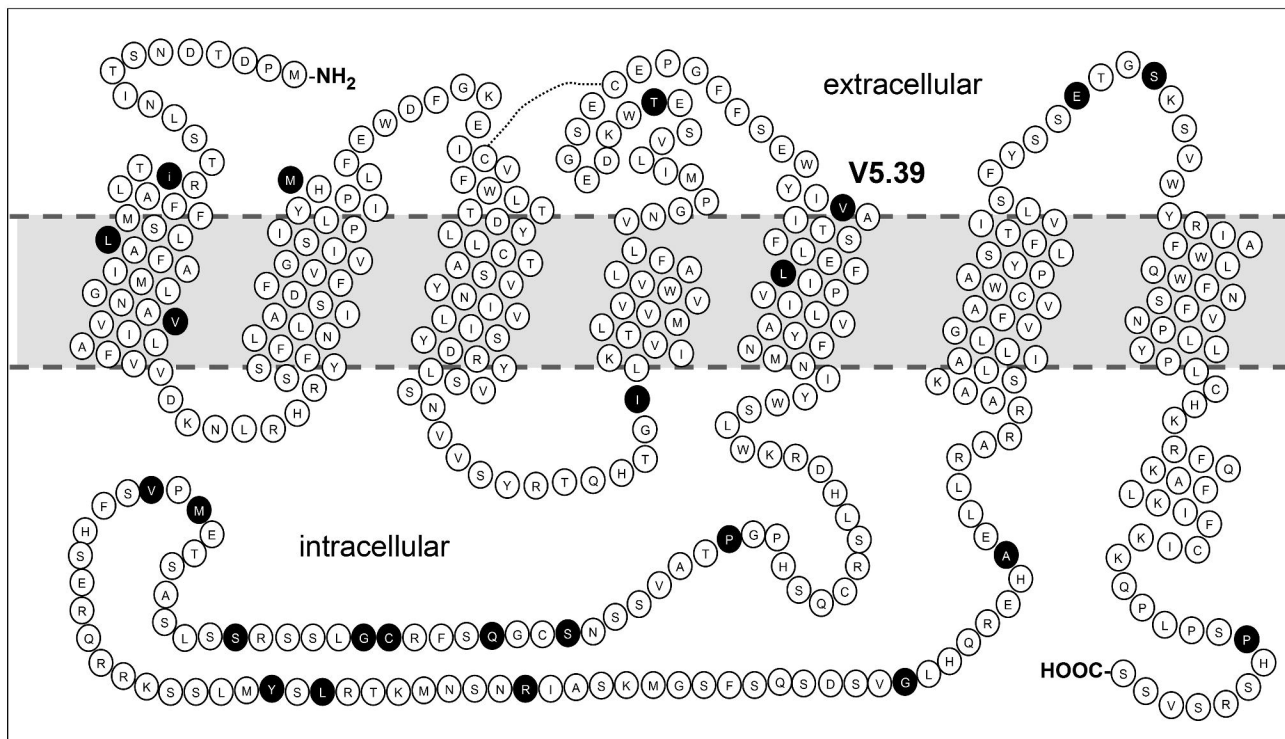


Figure 5

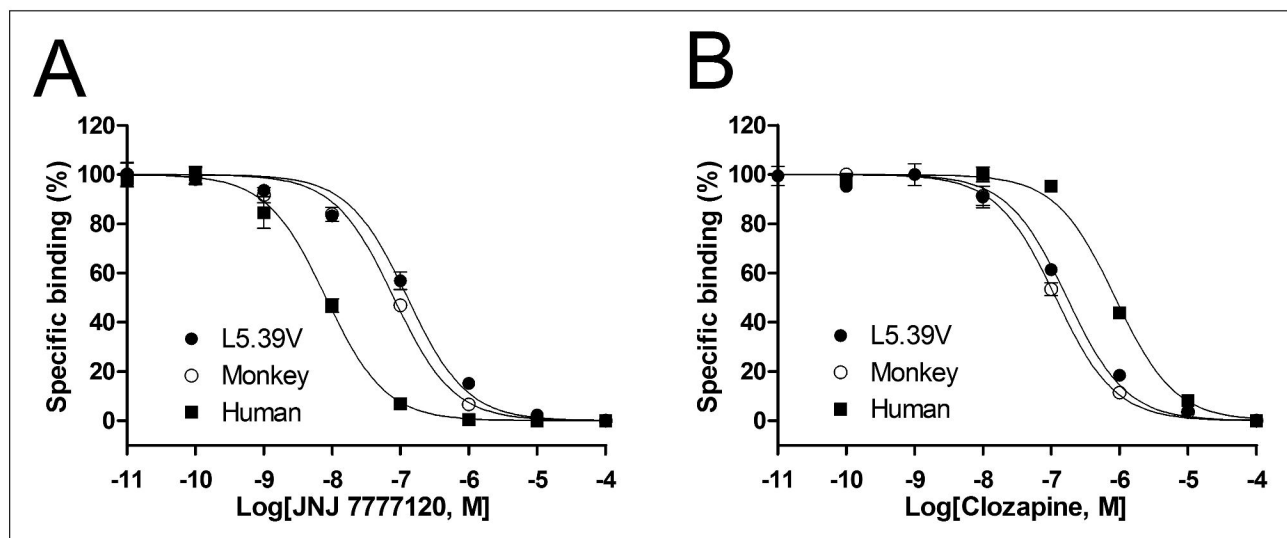


Figure 6

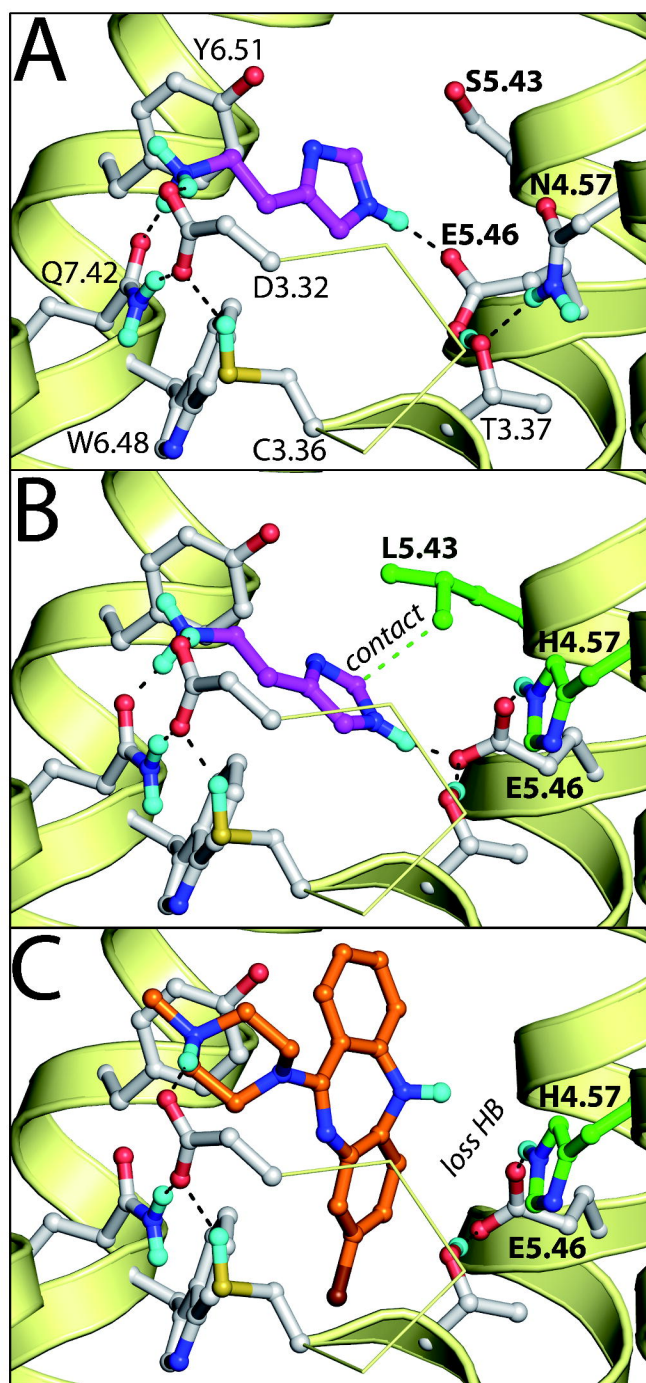


Figure 7

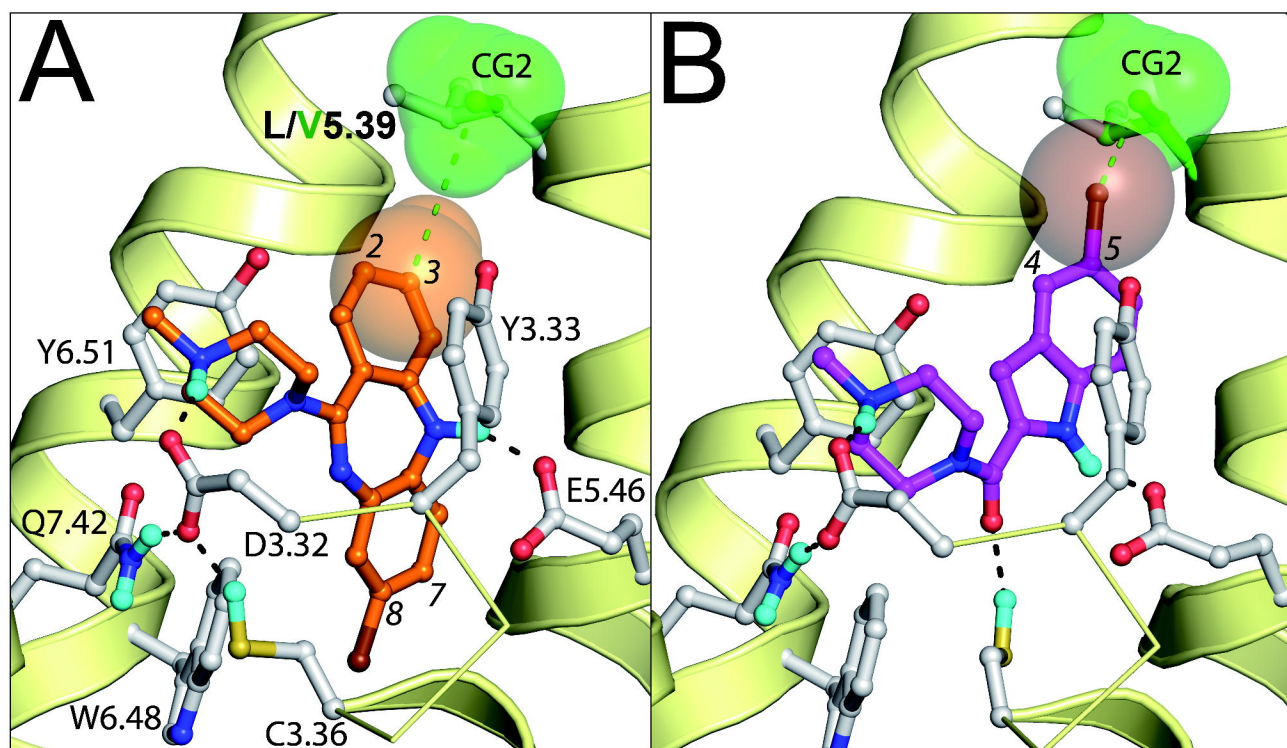


Figure 8